ONLINE SUPPLEMENT

Pharmacologically-induced thoracic and abdominal aortic aneurysms in mice

Yasuhisa Kanematsu, Miyuki Kanematsu, Chie Kurihara, Tsung-Ling Tsou, Yoshitsugu Nuki, Elena I Liang, Hiroshi Makino, Tomoki Hashimoto

Short Title
A new mouse model of aortic aneurysm

Department of Anesthesia and Perioperative Care, University of California, San Francisco, California, USA

Correspondence to: Tomoki Hashimoto, M.D. Department of Anesthesia and Perioperative Care, University of California, San Francisco, 1001 Potrero Avenue, No. 3C-38, San Francisco, CA 94110, USA. Phone: (415) 206-8958. Fax: (415) 206-8170; Email: hashimot@anesthesia.ucsf.edu.

Expanded Methods

All experiments were conducted in accordance with the guidelines approved by the University of California, San Francisco, Institutional Animal Care and Use Committee.

Measurement of blood pressure

Systolic blood pressure was measured at baseline, one, three, and six-week in animals that received phosphate buffered saline (PBS) (control) (n=10), beta-aminopropionitrile (BAPN) alone (n=10), angiotensin-II alone (n=10), or combination of angiotensin-II and BAPN (n=45). Systolic blood pressure was measured using a tail-cuff method (ADInstruments) as previously described.[1]

In our preliminary experiments, we encountered that C57BL/6J mice have high locomotor activity and resistance to restrain even after training for blood pressure measurements, as previously described.[2, 3] Therefore, we anesthetized the mice with isoflurane, and systolic blood pressure was measured at the steady state (after 15 minutes of equilibration with the end-tidal isoflurane concentration at 1.5%) using a tail-cuff system (ADInstruments) to avoid confounding effects of locomotion and excitement on blood pressure measurement. A minimum of 10 measurements were obtained from each mouse.

Tissue harvesting

Mice were anesthetized with 5% isoflurane. Left cardiac ventricles were perfused with cold PBS (10 ml) under physiologic pressure with an exit through the severed right atrium. Hearts and aortas (portion between the heart and the bifurcation of iliac artery) were harvested. Harvested tissues were frozen in OCT compound immediately.

Definition of thoracic aortic aneurysm and abdominal aortic aneurysm

Thoracic and abdominal aortic aneurysms were defined as a localized dilation of the aortic wall with maximal outside diameter greater than 50% of its adjacent intact portion of aorta, which is the same set of criteria used for human aortic aneurysms.[4, 5] Image analyses were performed, using ImageJ software (National Institutes of Health) to measure the outer diameter of the aortic wall.

Histological and immunohistochemical examination

Serial cross-sections (10 μm thick) from both thoracic and abdominal aortas were mounted on microscope slides (Fisher Scientific Co.). In each group, 3 to 6 animals were examined for histology and immunohistochemistry. Sections were stained with hematoxylin and eosin (H&E), Elastica van Gieson (EVG), Gomori's trichrome, and Oil red O for histochemical examination, elastin and collagen, smooth muscle fibers, and lipids, respectively. Other aortic cross-sections (10 μm thick) were prepared for immunohistochemical staining to identify pan-leukocytes, macrophages, helper T-lymphocytes, B-lymphocytes, endothelial cells, fibroblasts, smooth muscle cells, cell proliferation, and apoptosis.

The following reagents were used to detect specific cell types: rat monoclonal anti mouse CD45 (1:1000 dilution; 553076) for pan-leukocytes, rat monoclonal anti mouse CD68 (1:300; MCA1957; AbD Serotec) for macrophages, rat monoclonal anti mouse CD4 (1:250; 553043) for helper T-lymphocytes, rat monoclonal anti mouse CD19 (1:100; 553783) for B-lymphocytes, rat monoclonal anti mouse CD31 (1:250; 553370) for endothelial cells, rabbit polyclonal anti S100A4 Ab-8 (1:150; RB-1804-A1; Neomarkers/Lab Vision) for fibroblasts, rabbit polyclonal anti alpha smooth muscle actin (1:400; AB5694; Abcam) for smooth muscle cells, and rabbit polyclonal anti Ki67 (1:300, AB9260; Chemicon) for cell proliferation; these antibodies were purchased from BD Pharmingen, unless otherwise specified. The primary antibody was omitted for negative control.

Sections were fixed with cold acetone for 20 minutes, and endogenous peroxidases were quenched by incubating sections in 0.3% hydrogen peroxide in methanol. Sections were subsequently blocked with 10% normal serum from host species of the secondary antibody. Sections were incubated in primary antibody overnight at 4°C, followed by incubation with corresponding biotinylated secondary antibodies (Vector Laboratories) and with a complex of avidin-biotin-horseradish peroxidase (Vector Laboratories). Immunoreactivity was visualized by incubating the sections with 0.05% 3,3'-diaminobenzidine (DAB, Vector Laboratories). Nuclei were visualized by counterstaining with aqueous hematoxylin.

To identify the major type of inflammatory cells among pan-leukocytes positive cells, double immunofluorescence staining was also performed. The antibodies used were rabbit polyclonal anti CD45 (1:200; sc-25590; Santa Cruz Biotechnology, Inc.) for pan-leukocytes, and rat monoclonal anti mouse CD68 (1:300; MCA1957; AbD Serotec) for macrophages. Pan-leukocytes were observed with red fluorescent anti-rabbit IgG IgG (Alexa 594; A11012; Invitrogen), and macrophages were observed with fluorescein anti-rat IgG (Fluorescein; FI-4001; Vector laboratories). The images were visualized using fluorescence microscopy.

To assess apoptosis, terminal deoxynucleotidyl transferase-mediated dUTP-biotin nick end labeling (TUNEL) assay was performed using the ApopTag kit (S7101; ApopTag Peroxidase In Situ Oligo Ligation Apoptosis Detection Kit; Chemicon) according to the manufacturer's instructions. To assess cell proliferation, we stained the tissues with anti-Ki67 antibody.

Quantification of inflammatory cells in aortic wall, thickness of vascular wall, and degree of degeneration of elastic lamina

Two blinded observers independently performed quantitative analysis. Quantification of inflammatory cells was performed as previously described.[6] The thoracic and abdominal aorta or aortic aneurysm sections that were immunostained for CD45, CD68, CD4, and CD19, as mentioned above, were also used (n = 6 aortas). Positive-stained cells were counted at four different representative locations under high magnification (400x). The number of positive cells per area of 0.01 square millimeters was calculated using the following formula: number of positive cells per field / aortic area per field. The aortic area

per field was measured by using ImageJ software (National Institutes of Health). Results from the two observers were averaged. Thickness of aortic wall and grading of the degree of elastic lamina degeneration were analyzed by using H&E stained cross-sections of the thoracic and abdominal aortas or aortic aneurysms. Thickness of total wall, media, and adventitia at four different areas (every 90 degrees) per cross section in each aorta were measured and averaged (n = 6 aortas). The same samples were graded to quantify the severity of changes in the elastic lamina using the method as previously described by others.[7] The severity of changes in the elastic lamina was scored from 1 to 4; 1: completely intact elastic laminas, 2: mild degeneration (in less than 50% of area of the medial layers), 3: extensive degeneration or fragmentation (in more than 50% of area of the medial layers), and 4: complete disruption of the entire media as previously described.[7] Four different areas per cross section in each aorta were evaluated and averaged (n= 6 aortas).

Blood flow measurement

Blood flow rates of the thoracic aortas, abdominal aortas, and common carotid arteries in non-transplanted mice, and grafted thoracic aortas and abdominal aortas in transplanted mice were measured using an ultrasound transit-time probe (Transonic Systems) as previously described.[8, 9] All measurements were performed six weeks after the initiation of treatment with or without angiotensin-II and BAPN (seven weeks after transplantation).

Mice were anesthetized with 1.5% isoflurane. Mice were intubated and ventilated using a small animal ventilator (Harvard Apparatus). Tidal volume of the pump was set at 0.4 ml, and the respiratory rate was set at 120 strokes per minute. A median sternotomy was performed, and a modified retractor was inserted to visualize the heart and the ascending aorta. Dissection along the ascending aorta was performed to free the vessel from the surrounding connective tissues. 1.5 PSL flow probe was placed under the aorta, and blood flow signal was recorded and analyzed with the PowerLab System using Chart 5 software (ADInstruments). For the measurement of abdominal aortic blood flow, a midline laparotomy was performed. Suprarenal abdominal aorta was exposed, and blood flow was measured.

Expanded Results

Time course of aneurysm formation and growth

To assess the time course of aneurysm formation and growth in this model, we prepared additional mice that were treated with angiotensin-II and BAPN and sacrificed them at two-weeks (n=10). As shown in **Supplemental Figure S1A**, incidence of thoracic aortic aneurysms was 30% and 38% at two and six-weeks, respectively. **Supplemental Figure S1B** shows an increase in the mean outer diameter of the thoracic aorta from control to two-weeks and two-weeks to six-weeks, suggesting continuous growth of thoracic aortic aneurysm over the six-week period (control vs. six-weeks: 0.92 ± 0.09 vs. 1.58 ± 0.54 mm, $P<0.05$; two-weeks vs. six-weeks: 1.23 ± 0.25 vs. 1.58 ± 0.54 mm, $P <0.05$).

In contrast, there was no difference in incidence of abdominal aortic aneurysms between two-weeks and six-weeks (50% vs. 49%) **(Supplemental Figure S1A)**. However, similar to the thoracic aorta, the mean outer diameter of the abdominal aorta gradually increased from control to two-weeks, and two-weeks to six-weeks, suggesting continuous growth of aneurysm over the six-week period (control vs. six-weeks: 0.74 ± 0.04 vs. 1.77 ± 0.95 mm, $P <0.05$) **(Supplemental Figure S1B)**. Possibly due to the faster rate of abdominal aortic aneurysm growth relative to that of thoracic aortic aneurysm, the incidence of abdominal aortic aneurysms reached plateau at two-weeks. There appeared to be discrepancies between the incidence of abdominal aortic aneurysms and the outer diameter. While there was continuous growth of the outer diameter between two and six-weeks, there was no difference in incidence of abdominal aortic aneurysms during that same period. This was thought to be due to the dichotomous nature of the diagnostic criteria that used an arbitrary cutoff at 50% increase of diameter to define as aneurysms. While both thoracic and abdominal aortic aneurysms appeared to continuously grow over the six-week period, more abdominal aortic aneurysms than thoracic aortic aneurysms reached the 50% increase cutoff within two-weeks **(Supplemental Figure S1C)**. Localized dilation of the aorta that did not reach the 50% cutoff may be considered as pre-aneurysmal lesions. As described below, histological assessment of these pre-aneurysmal lesions showed similar histological changes to those of aneurysm tissues **(Supplemental Figure S3)**.

Interestingly, none of the distal descending thoracic aortic samples, except for the two small isolated aneurysms that developed, showed significant increase in the outer diameter over the six-week period **(Supplemental Figure S1B)**. There were no differences in the mean outer diameter of the distal descending thoracic aorta among the time points studied. These data may indicate that the distal descending thoracic aorta have different responses to the combination of angiotensin-II and BAPN compared to the thoracic and abdominal aortas, which were two regions of the aorta where the majority of aneurysms were found.

Oil red O staining to assess early atherosclerotic changes

Oil red O staining showed a presence of lipids around the intramural thrombus in abdominal aortic aneurysm (arrows indicate the positive staining of

lipids), possibly an early sign of atherosclerosis **(Supplemental Figure S2B)**. However, atherosclerotic changes were not found in thoracic aortic aneurysm in our model **(Supplemental Figure S2A)**.

Aortic wall with pre-aneurysmal changes at one-week and six-weeks

At one-week time point, histological changes started in both ascending and abdominal aorta, such as increase of fibroblasts, disorganization of medial layers, and accumulation of numerous inflammatory cells **(Supplemental Figure S3)**. In both six-week aortas, these pre-aneurysmal changes developed more severely, in spite of lack of macroscopic aneurysm formation **(Supplemental Figure S3)**. Unlike aneurysm samples, complete medial break or intramural thrombus was not found in aortas with pre-aneurysmal changes.

Morphometric analysis of different stages of thoracic and abdominal aortic aneurysms

Damages of the elastic lamina and accompanied changes in the media were more pronounced in the thoracic aortas than in the abdominal aortas. In addition, the thoracic and abdominal aortas revealed different time course of changes in wall thickness and in severity of damages of the elastic laminas.

In thoracic aortas, the total wall thickness gradually increased from control to one-week, to two-weeks, and to six-weeks **(Supplemental Figure S4A, left)**. The gradual increase in wall thickness of the thoracic aorta was mainly due to the gradual thickening of the media, which was accompanied by the gradual increase in the severity of the damages in the elastic lamina **(Supplemental Figure S4B, left)**. The time course of increase in the wall thickness and media in the thoracic aorta was similar to the time course of increase in the outer diameter **(Supplemental Figure S1B)**, indicating that the gradual increase in outer diameter over the six-week period was mainly due to the increase in wall thickness.

In contrast, the increase in thickness of the vascular wall, media, and adventitia of the abdominal aorta reached a plateau at one-week, except for the region of the vascular wall with intramural thrombus (w IMT) **(Supplemental Figure S4A right)**. Similarly, severity of damages in the elastic lamina reached plateau at one-week **(Supplemental Figure S4B right)**. Faster rate of change in the wall thickness of the abdominal aortas coincided with faster rate of growth of the outer diameter presented in **Supplemental Figure S1B**.

Inflammatory cell infiltration

Double staining for CD45 (pan-leukocytes) and CD68 (macrophages) in aortic aneurysm tissues showed that the majority of pan-leukocytes in thoracic aortic aneurysms were macrophages **(Supplemental Figure S5A)**.

Semi-quantification of leukocytes at different stages of aneurysm formation is presented in **Supplemental Figure S5B**.

Cell proliferation and apoptosis

Concurrent proliferation and apoptosis of vascular cells were observed in human aortic aneurysms.[10, 11] Therefore, terminal deoxynucleotidyl transferase-mediated dUTP-biotin nick end labeling (TUNEL) and Ki67 staining were employed for assessment of apoptosis and proliferation, respectively **(Supplemental Figure S6)**. At all time points we studied, abundant TUNEL positive cells were detected in both media and adventitia, regardless of whether aneurysms formed. However, there were far less Ki67 positive cells than TUNEL positive cells, indicating possible imbalance between the processes of cell proliferation and apoptosis.

Supplemental References

1. Weiss D, Kools JJ, Taylor WR. Angiotensin II-induced hypertension accelerates the development of atherosclerosis in apoE-deficient mice. *Circulation.* 2001;103:448-454.
2. Daugherty A, Manning MW, Cassis LA. Angiotensin II promotes atherosclerotic lesions and aneurysms in apolipoprotein E-deficient mice. *J Clin Invest.* 2000;105:1605-1612.
3. Davis WM, King WT. Pharmacogenetic factor in the convulsive responses of mice to flurothyl. *Experientia.* 1967;23:214-215.
4. Johnston KW, Rutherford RB, Tilson MD, Shah DM, Hollier L, Stanley JC. Suggested standards for reporting on arterial aneurysms. Subcommittee on Reporting Standards for Arterial Aneurysms, Ad Hoc Committee on Reporting Standards, Society for Vascular Surgery and North American Chapter, International Society for Cardiovascular Surgery. *J Vasc Surg.* 1991;13:452-458.
5. Kato K, Oguri M, Kato N, Hibino T, Yajima K, Yoshida T, Metoki N, Yoshida H, Satoh K, Watanabe S, Yokoi K, Murohara T, Yamada Y. Assessment of genetic risk factors for thoracic aortic aneurysm in hypertensive patients. *Am J Hypertens.* 2008;21:1023-1027.
6. Zhang Y, Ramos KS. The development of abdominal aortic aneurysms in mice is enhanced by benzo(a)pyrene. *Vasc Health Risk Manag.* 2008;4:1095-1102.
7. Habashi JP, Judge DP, Holm TM, Cohn RD, Loeys BL, Cooper TK, Myers L, Klein EC, Liu G, Calvi C, Podowski M, Neptune ER, Halushka MK, Bedja D, Gabrielson K, Rifkin DB, Carta L, Ramirez F, Huso DL, Dietz HC. Losartan, an AT1 antagonist, prevents aortic aneurysm in a mouse model of Marfan syndrome. *Science.* 2006;312:117-121.
8. Scherrer-Crosbie M, Steudel W, Hunziker PR, Foster GP, Garrido L, Liel-Cohen N, Zapol WM, Picard MH. Determination of right ventricular structure and function in normoxic and hypoxic mice: a transesophageal echocardiographic study. *Circulation.* 1998;98:1015-1021.
9. Theodorakis NG, Wang YN, Skill NJ, Metz MA, Cahill PA, Redmond EM, Sitzmann JV. The role of nitric oxide synthase isoforms in extrahepatic portal hypertension: studies in gene-knockout mice. *Gastroenterology.* 2003;124:1500-1508.
10. He R, Guo DC, Estrera AL, Safi HJ, Huynh TT, Yin Z, Cao SN, Lin J, Kurian T, Buja LM, Geng YJ, Milewicz DM. Characterization of the inflammatory and apoptotic cells in the aortas of patients with ascending thoracic aortic aneurysms and dissections. *The Journal of thoracic and cardiovascular surgery.* 2006;131:671-678.
11. Thompson RW, Geraghty PJ, Lee JK. Abdominal aortic aneurysms: basic mechanisms and clinical implications. *Curr Probl Surg.* 2002;39:110-230.

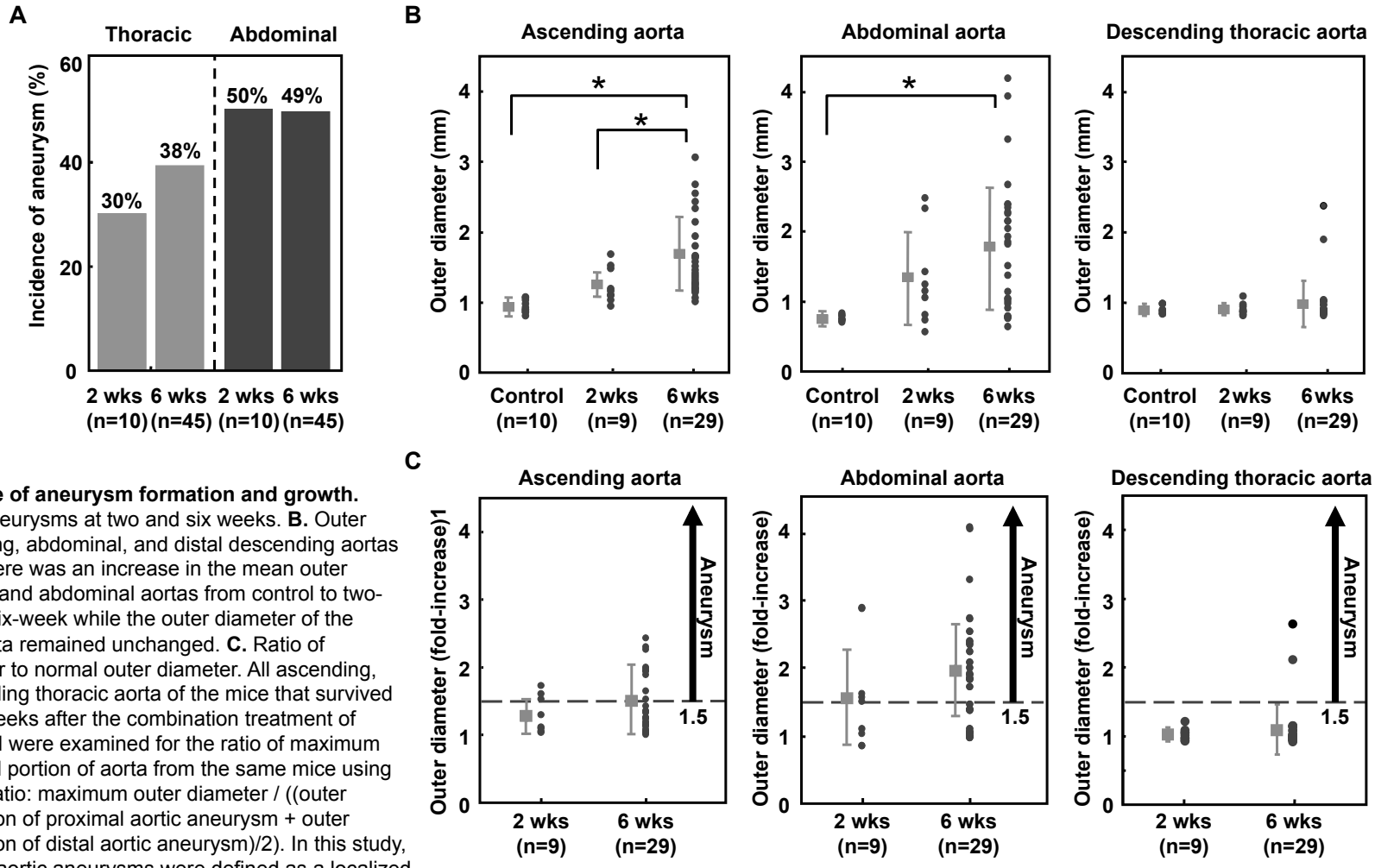

Figure S1. Time course of aneurysm formation and growth. **A.** Incidence of aortic aneurysms at two and six weeks. **B.** Outer diameter of the ascending, abdominal, and distal descending aortas at two and six-week. There was an increase in the mean outer diameter of the thoracic and abdominal aortas from control to two-week and two-week to six-week while the outer diameter of the descending thoracic aorta remained unchanged. **C.** Ratio of maximum outer diameter to normal outer diameter. All ascending, abdominal, and descending thoracic aorta of the mice that survived for two weeks and six weeks after the combination treatment of angiotensin-II and BAPN were examined for the ratio of maximum outer diameter to normal portion of aorta from the same mice using the following formula. Ratio: maximum outer diameter / ((outer diameter in normal portion of proximal aortic aneurysm + outer diameter in normal portion of distal aortic aneurysm)/2). In this study, thoracic and abdominal aortic aneurysms were defined as a localized dilation of the aortic wall with maximal outside diameter greater than 50% of its adjacent intact portion of aorta, which is the same criteria used for human aortic aneurysms.4, 5 Mean ± SD. *: $P < 0.05$.

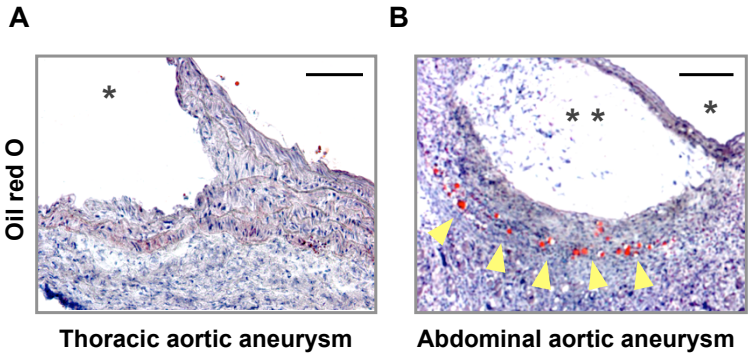

Figure S2. Examination for lipids in aortic aneurysms. To assess presence of atherosclerotic changes, oil red O stating was used to detect lipids. Oil red O staining showed a presence of lipids around the intramural thrombus in abdominal aortic aneurysm (arrows indicate the positive staining of lipids), possibly an early sign of atherosclerosis. But atherosclerotic changes were not found in thoracic aortic aneurysm in our model. Scale bars: 0.1mm. *: lumen; **: intramural thrombus.

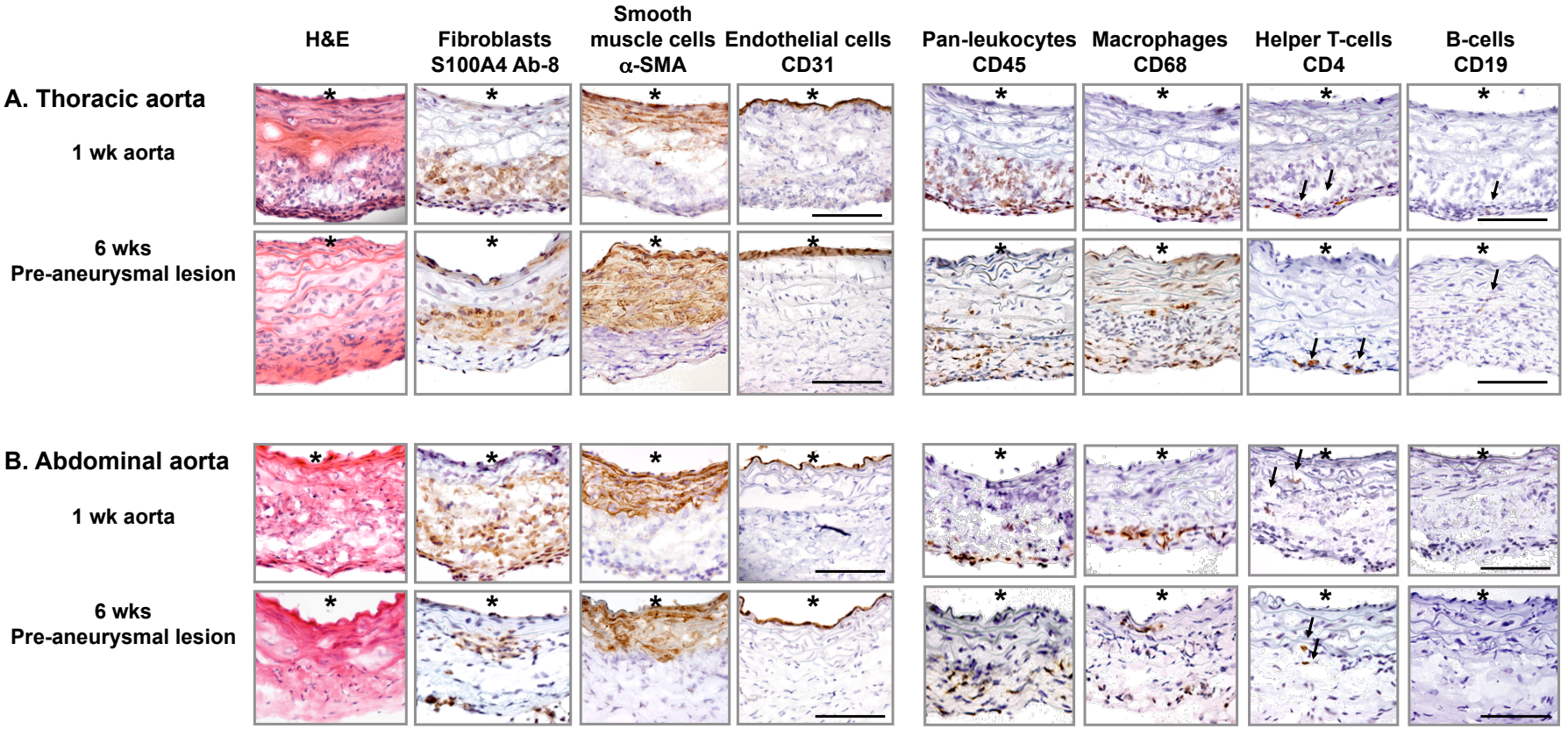

Figure S3. Pre-aneurysmal changes in aortas without mature aneurysm formation at one-week and six-week. Representative stainings for H&E, fibroblasts (S100A4 Ab-8), smooth muscle cells (alpha smooth muscle actin), endothelial cells (CD31), pan-leukocytes (CD45), macrophages (CD68), Helper T-lymphocytes (CD4) and B-lymphocytes (CD19) in **(A)** thoracic aortas and **(B)** abdominal aortas without mature aneurysm formation (pre-aneurysmal lesion) at one and six-week time point. At one-week time point, histological changes started in both ascending and abdominal aorta, such as increase of fibroblasts, disorganization of medial layers, and accumulation of numerous inflammatory cells. In six-week aortas, these pre-aneurysmal changes developed severer in spite of lack of macroscopic aneurysm formation. Unlike aneurysm samples, complete medial break or intramural thrombus was not found in aortas with pre-aneurysmal changes. Scale bars: 0.1mm. *: lumen; arrows indicate positive cells.

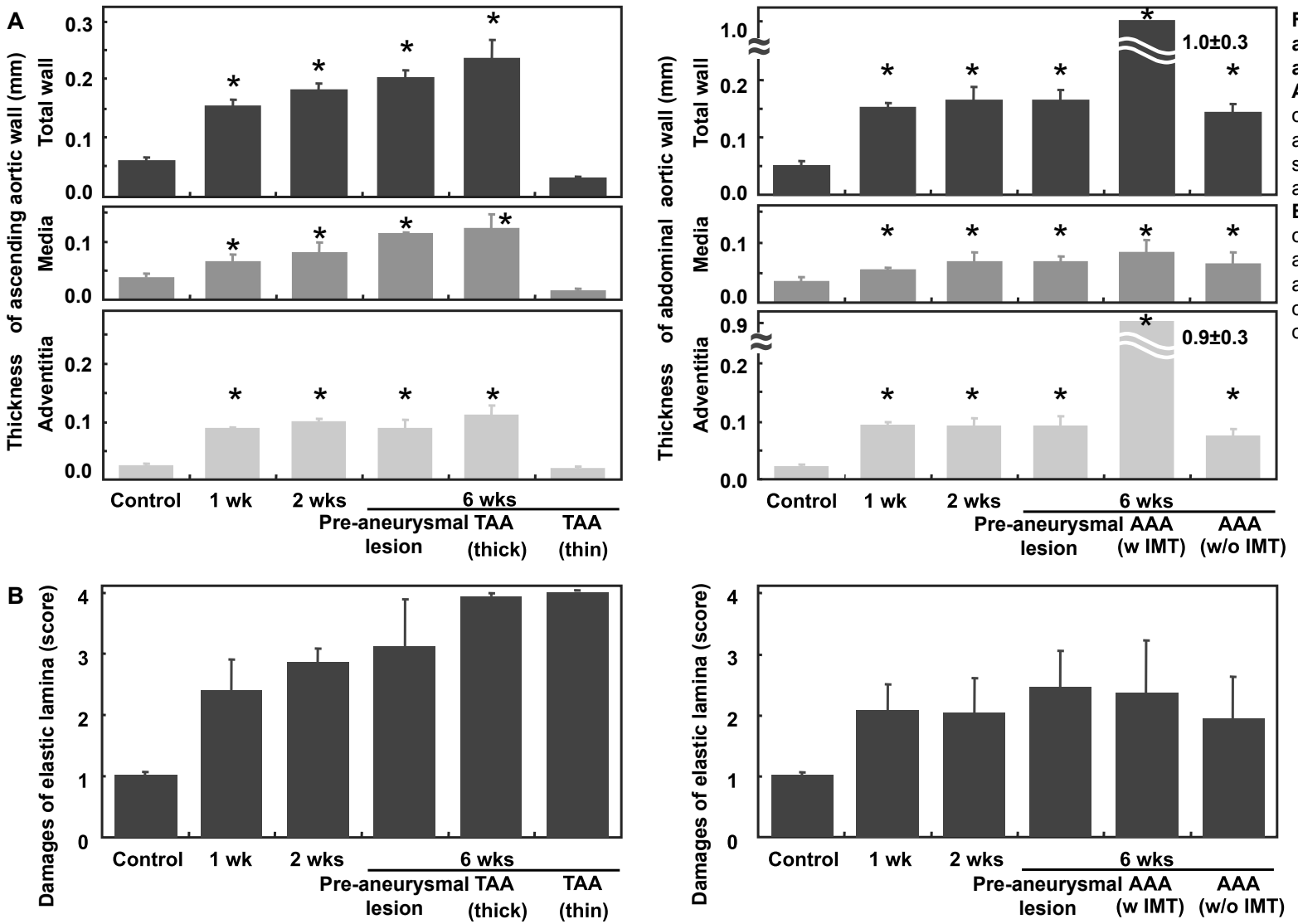

Figure S4. Morphometric analysis of thoracic and abdominal aortic aneurysms. **A.** Quantification of thickness of the vascular wall, media, and adventitia at different stages of thoracic and abdominal aortic aneurysms. **B.** Grading of the degeneration of elastic lamina. TAA: thoracic aortic aneurysm; AAA: abdominal aortic aneurysm; w or w/o IMT: the aortic wall with or without

A

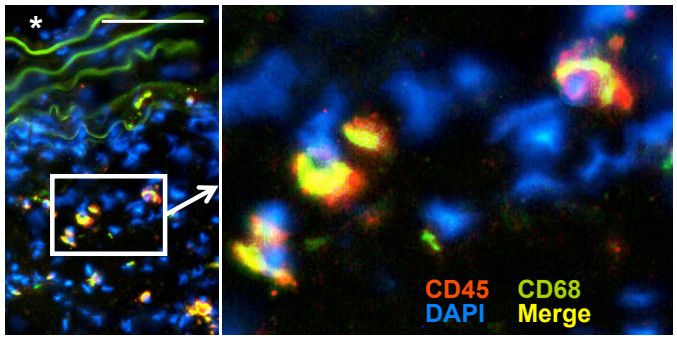

Figure S5. Inflammatory cell infiltration in aortic aneurysms.
A. Representative images of double immunofluorescent staining for macrophages (CD68 positive cells) and pan-leukocytes (CD45 positive cells) in aortic aneurysm at six-week time point are shown. The majority of pan-leukocytes in thoracic aortic aneurysms were macrophages. **B.** Quantification of inflammatory cells. TAA: thoracic aortic aneurysm; AAA: abdominal aortic aneurysm; w or w/o IMT: the aortic wall with or without intramural thrombus. Scale bars: 0.1mm. *:

B

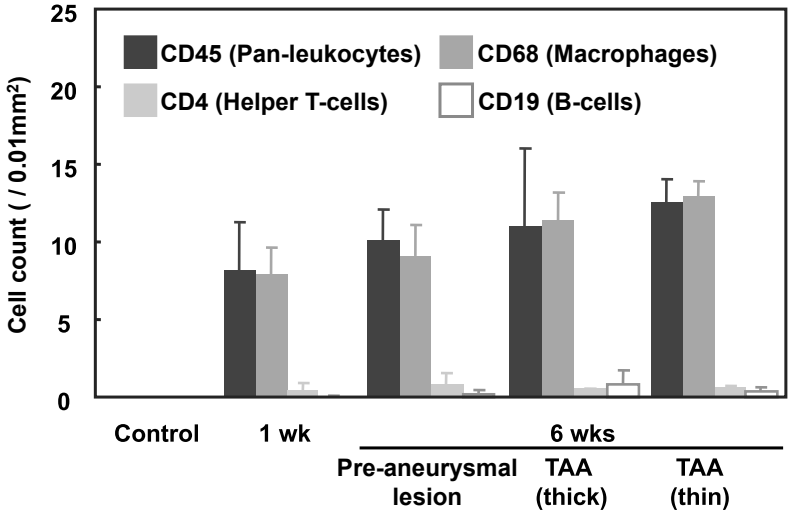

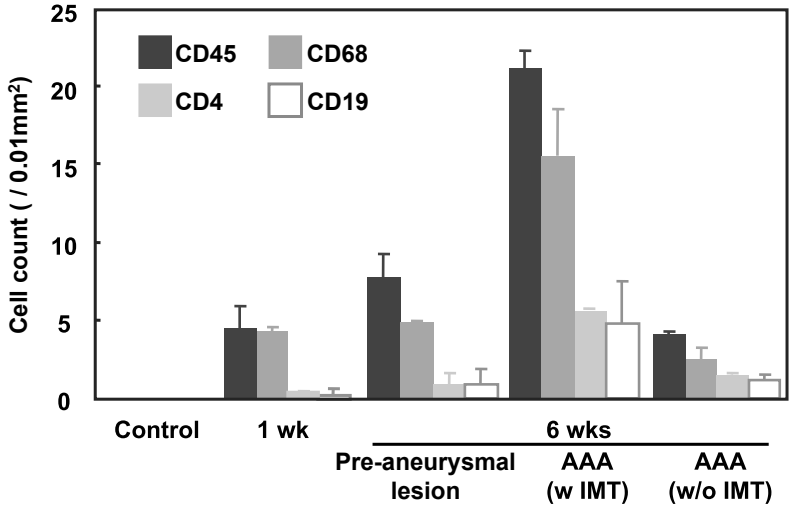

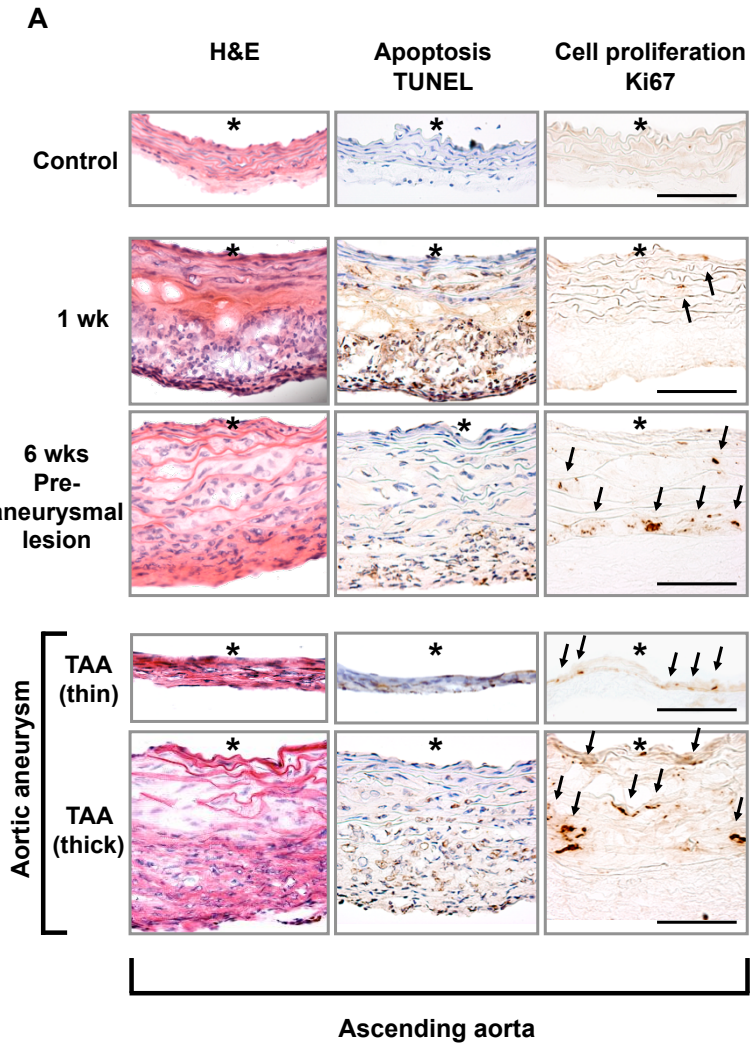

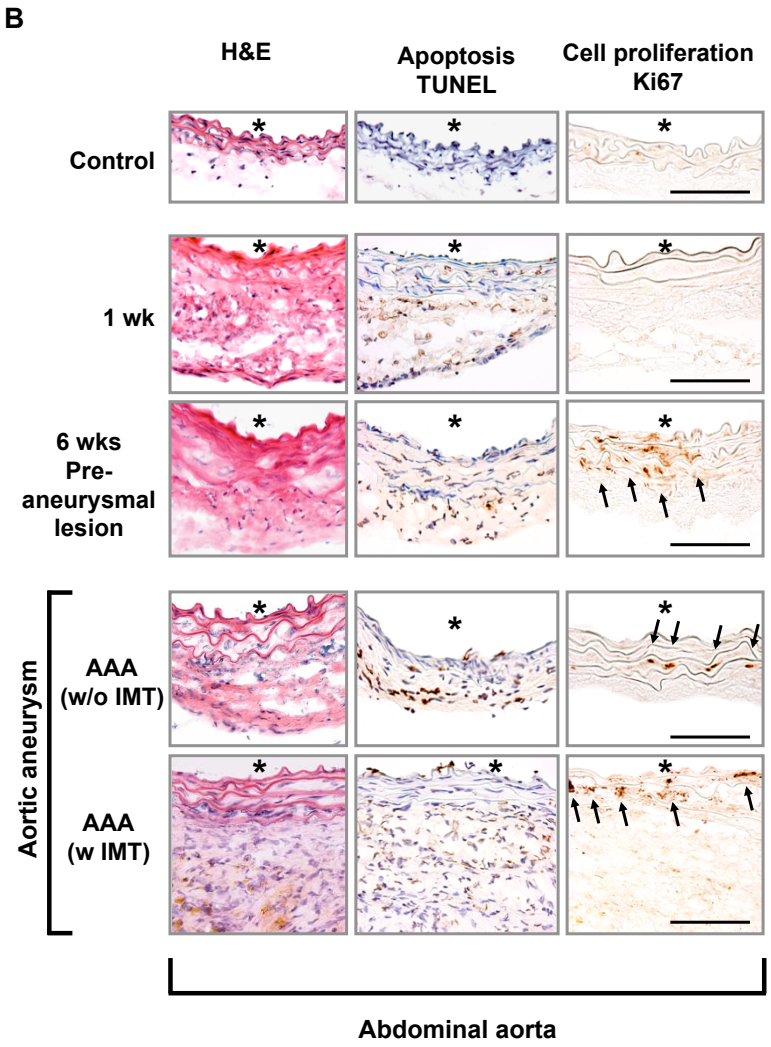

Figure S6. Apoptosis and cell proliferation in aortic aneurysms. Terminal deoxynucleotidyl transferase-mediated dUTP-biotin nick end labeling (TUNEL) and Ki67 staining were employed for assessment of apoptotic and proliferating cells, respectively. Both the thoracic and abdominal aortas with pre-aneurysmal changes showed abundant TUNEL positive cells in the adventitia and media as early as one-week time point. However, very few Ki67 positive cells were detected in both regions of aortas at one-week. At six-week time point after the treatment with angiotensin-II and BAPN, many Ki67 positive cells were detected in the smooth muscle cell layer of thoracic and abdominal aortas, regardless of whether aneurysm formed. TAA: thoracic aortic aneurysm; AAA: abdominal aortic aneurysm; w or w/o IMT: the aortic wall with or without intramural thrombus. Scale bars: 0.1mm. *: lumen; Arrows indicate positive cells.